

# Hydroxyapatite Nanoceramic Thick Film: An Efficient CO<sub>2</sub> Gas Sensor

R.U. Mene<sup>1</sup>, M.P. Mahabole<sup>1</sup>, R.C. Aiyer<sup>2</sup> and R.S. Khairnar<sup>1,\*</sup>

<sup>1</sup>School of Physical Sciences, S.R.T.M. University, Nanded 431 606, India

<sup>2</sup>Department of Physics, Pune University, Pune-411 007, India

**Abstract:** Hydroxyapatite (HAp) is widely used in biomedical applications due to its superb bioactive behavior. Moreover, it possesses potential applications in varied fields like chromatography, catalyst, fuel cell & chemical gas sensor. The hydroxyapatite thick films were deposited on insulating substrate using screen printing technique. The phase composition and particle morphology of the films were examined by means of X-ray diffraction and Scanning Electron Microscopy respectively. Energy Dispersive Spectroscopic study confirmed the elemental composition of the hydroxyapatite thick films. A systematic study on CO<sub>2</sub> gas sensing was carried out to determine operating temperature of hydroxyapatite thick film sensor. Effect of gas concentration on sensitivity factor and other parameters such as response and recovery time of HAp thick film for CO<sub>2</sub> were also investigated. The study revealed that HAp thick film is an excellent sensor for the detection of CO<sub>2</sub> gas at 165°C which is relatively lower operating temperature as compared to CO<sub>2</sub> gas sensors available in the market today.

**Keywords:** Hydroxyapatite, thick films, gas sensor, screen printing technique, SEM/EDS.

## 1. INTRODUCTION

Recent technological developments have brought along with them several environmental problems like air pollution, industrial pollution etc. Due to stringent regulations governing air pollution, it is important to focus sensor research on the development of new low-cost gas sensor materials, having high sensitivity, selectivity, fast response and stability. Most of the sensor work is concentrated on semiconducting oxides like ZnO, SnO<sub>2</sub>, TiO<sub>2</sub>, CuO [1], due to their sensitive nature over the wide temperature range and also on polymer and ferrite material. However, comparatively less attention has been directed towards the use of ceramic materials, especially nanoceramic hydroxyapatite, as a gas sensor. Hydroxyapatite [HAp, Ca<sub>10</sub>(PO<sub>4</sub>)<sub>6</sub>(OH)<sub>2</sub>], which belongs to inorganic bioceramic category, is extensively used in biomedical applications due to its bioactive nature [2]. In addition, HAp has also been used successfully as an adsorbent for separation of proteins and enzymes [3], adsorption of bovine serum albumin [4] catalyst [5], drug delivery system [6] and fuel cell [7]. Moreover, HAp surface possesses several P-OH groups which act as adsorption sites for various molecules such as H<sub>2</sub>O, CH<sub>3</sub>OH, & CH<sub>3</sub>I [8, 9]. Furthermore, the nanosize and porous nature of HAp plays a vital role for adsorption of a large number of chemical gases. Considering the above facts and assets of HAp, the CO gas sensing properties of HAp ceramic, operating at a lower temperature of 125°C, has been reported by our group [10-12]. Nagai *et al.* have also developed porous HAp thick film gas sensor, using electrical conductivity measurements in air and CO<sub>2</sub>

gas atmosphere at 400°C [13]. FTIR study of adsorption of a CO<sub>2</sub> on calcium hydroxyapatite has carried out by cheng *et al.* [14] *et al.* have reported the use of silica-hydroxyapatite films as a biosensor for the detection of hydrogen peroxide [15].

Literature survey reveals that meager work is carried out in case of HAp nano-ceramic as a gas sensor. Hence, the efforts have been carried out for the development of CO<sub>2</sub> gas sensor based on HAp matrix.

Therefore, the present investigation reports a detailed study on gas sensing properties of screen printed HAp thick film prepared using nano crystalline synthetic HAp and its characterization by SEM/EDS, and XRD. It also deals with the detail investigation on repeatability & reproducibility of the film, determination of response & recovery times and active region of HAp sensor for CO<sub>2</sub> gas.

## 2. MATERIALS AND METHODOLOGY

### 2.1. Material Synthesis

Hydroxyapatite nano-ceramic was prepared using wet chemical process as reported earlier (10). Merck grade calcium nitrate, di-ammonium hydrogen phosphate, liquid ammonia were used as the starting chemicals. Calcium nitrate and di-ammonium hydrogen orthophosphate solutions were prepared so as to get theoretical Ca/P ratio close to 1.66. Slow drop wise addition of di-ammonium hydrogen phosphate solution in to calcium nitrate solution was followed by continuous stirring for about 3 hours at a temperature 100°C. The pH of the reaction was adjusted by the addition of NH<sub>4</sub>OH. The resulting white precipitate was washed thoroughly with double distilled water and dried in air oven at 100°C and finally sintered at 1000°C for 2 hours.

\*Address correspondence to this author at the School of Physical Sciences, S.R.T.M. University, Nanded 431 606, India; Tel: +91-2462-229559; Fax: +91-2462-229559; E-mail: rskhairnar.srtmun@gmail.com, rskhairnar@srtmun.ac.in

## 2.2. Thick Film Preparation

Screen printing technique was used to deposit HAp thick films on alumina substrate due to ease of fabrication, compactness, low cost and robustness [16, 17]. The paste was prepared by homogeneous mixing of HAp (functional material), lead borosilicate glass (permanent binder) butyl carbitol acetate & ethyl cellulose (temporary binders). The ratio of inorganic to organic part was kept as 70:30 for getting thixotropic properties of the paste. The alumina substrates were cleaned by using soap solution, chromic acid and distilled water followed by ultrasonic treatment (20 min). The paste was deposited on pre-cleaned (reduce the space between two words) insulating substrate (with dimensions 10 mm x 10 mm) by means of screen printing technique. All the films used in the experimentation were composed of two layers. The screen printed films were dried under IR lamp at 100°C for 20 min followed by sintering at elevated temperatures in the range of 600°C- 800°C to ensure better adhesion and to remove temporary organic binders. The best adhesion was found for the films sintered at 750°C for 1 hour & these films were used as sensor samples for further studies.

## 2.3. Characterization

### 2.3.1. X-ray Diffraction

The XRD analysis of the film was carried out for HAp phase identification. X-ray diffraction pattern was recorded with a Rigaku make X-ray diffractometer (Miniflex) with  $\text{CuK}\alpha$  ( $\lambda = 1.543 \text{ \AA}$ ) incident radiation. The XRD peaks were recorded in the  $2\theta$  range of 20°–80°.

### 2.3.2. Scanning Electron Microscopy (SEM) and Energy Dispersive Spectroscopy (EDS)

Scanning Electron Microscope (JSM/JEOL model no.-6360) was used to observe the surface morphology and microstructure of the HAp films deposited on alumina. Thin film of gold (Au) was deposited on HAp thick film to reduce charging of the sample. Simultaneous EDS study was carried out using 6360(LA) instrument. The experiment was performed at an accelerating voltage of 20 kV & probe current of 1nA with counting rate 9755 cps & energy range 0-20 keV.

## 2.4. Gas Sensing Characterization

The static gas characterization system was used to study the gas sensing properties of HAp thick films. To avoid the relative humidity effect, the preheated samples were used for the experimentation. The DC voltage of 90 V ( $V_s$ ) was applied across the film and voltage drop ( $V_r$ ), across reference resistance ( $R_r$ ), was measured at the selected interval of temperature. The resistance of the thick film in air,  $R_{\text{sensor}}$  ( $R_s$ ), was determined by using the following formula.

$$R_s = \{[V_s - V_r]/V_r\} R_r \quad (1)$$

The required gas concentration inside the system was achieved by injecting a known volume of the test gas and the change in resistance of the sensor thick film ( $R_g$ ), as a function of temperature, was also determined using equation (1). The percentage sensitivity factor (SF(%)) was calculated by using the following formula;

$$\text{SF}(\%) (R) = [R_g - R_a] / R_a * 100 = (\Delta R / R_a * 100) \quad (2)$$

OR

$$\text{SF}(\%) (G) = [G_g - G_a] / G_a * 100 = (\Delta G / G_a * 100) \quad (3)$$

Where,  $R_a$ ,  $R_g$ ,  $G_a$ , &  $G_g$  were the resistance and conductance of the sensor film in air and in gas respectively.

The study on  $\text{CO}_2$  gas sensing properties of hydroxyapatite was carried out for various  $\text{CO}_2$  gas concentrations, viz, 1 ppm, 10 ppm, 100 ppm, 1000 ppm and 10000 ppm. Small change in resistance was observed for gas concentration of 500 ppm but with a response time of the order of 2 min 30 second. Where as for 1000 ppm  $\text{CO}_2$  concentration, the response time of the order of 20 seconds was observed. Thus a gas load of 1000 ppm was fixed for further study of gas sensing experimentation.

The film was exposed to 1000 ppm gas and sensitivity factor was determined by heating the sensor film, from room temperature to elevated temperature. This experiment was repeated at least three to four times usually called as 'cycles' or 'run' for the same film, so as to assess the performance of repeatability from the point of view of, HAp thick film as a sensor device. To assess the reproducibility of sensor performance another sensor film (Film 2) was subjected to air-gas exposure for five times and SF%(R) as a function of temperature was determined. Further, the active range of gas sensing was optimized by introducing the sensor to variable gas concentration & thereby determining the effect on sensitivity factor. The response and recovery times are important parameters for commercial applications of sensor material. They are generally defined as the time taken for the sensor to attain 90% of maximum change in resistance upon exposure to gas and time taken by the sensor to get back 90% to the original resistance. Therefore, the response and recovery time were determined by exposing the sensor films to 1000 ppm gas and later to air alternately for number of cycles.

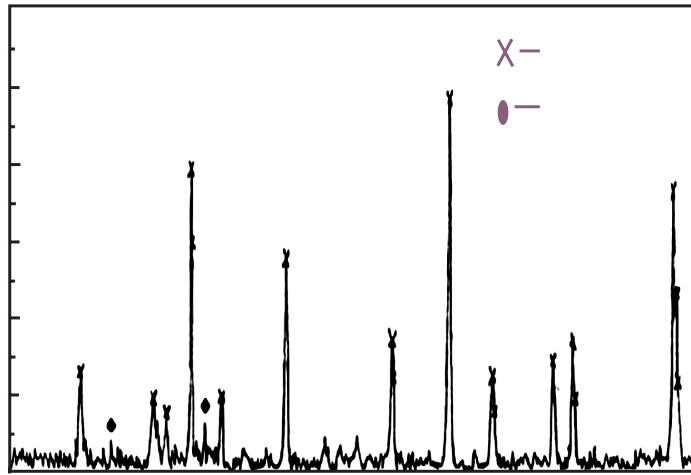
## 3. RESULTS AND DISCUSSION

### 3.1. X-ray Diffraction Studies

Fig. (1) shows the XRD pattern of the HAp thick film up to  $2\theta$  value of 20°–80°. The phase identification was performed by using JCPDS standard XRD card (09-432) for Hydroxyapatite. The presence of characteristic HAp peaks (x) indicates the confirmation of the HAp phase. The occurrence of two small intensity peaks, denoted by (●), indicate the presence of the binder material. The binder material, which was a borosilicate glass, may get crystallize locally during sintering of the films. Sintering process was essential to desorb the impurities and to have better adhesion and homogeneity in thick films [16, 17]. The crystallite size in the range of 58-60 nm was found for sintered thick films as calculated by Scherer's formula.

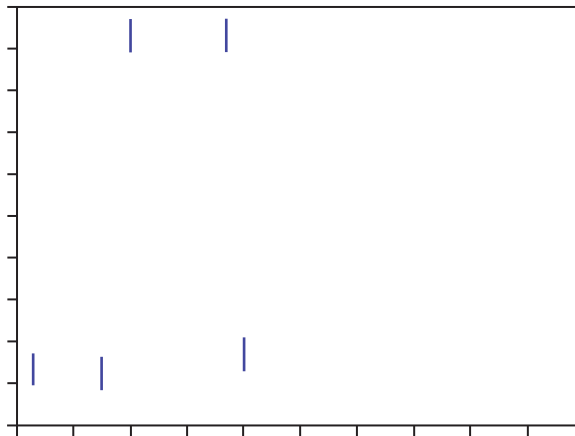
### 3.2. SEM/EDS Analysis

Fig. (2) shows SEM picture of sintered HAp thick film which was taken to visualize the general surface topography as well as presence of micro cracks and agglomerates. Energy dispersive spectroscopic (EDS) analysis, presented in Fig. (3), revealed that the main elements of the hydroxyapatite film are carbon, oxygen, aluminium, phosphorus and



**Fig. (1).** Typical XRD pattern of HAp thick film deposited on alumina & sintered at 750°C; x: peaks due hydroxyapatite & ●: peaks due to glass frit.

**Fig. (2).** Scanning electron micrograph of HAp thick film.



**Fig. (3).** Energy Dispersive Spectroscopic analysis of HAp thick film.

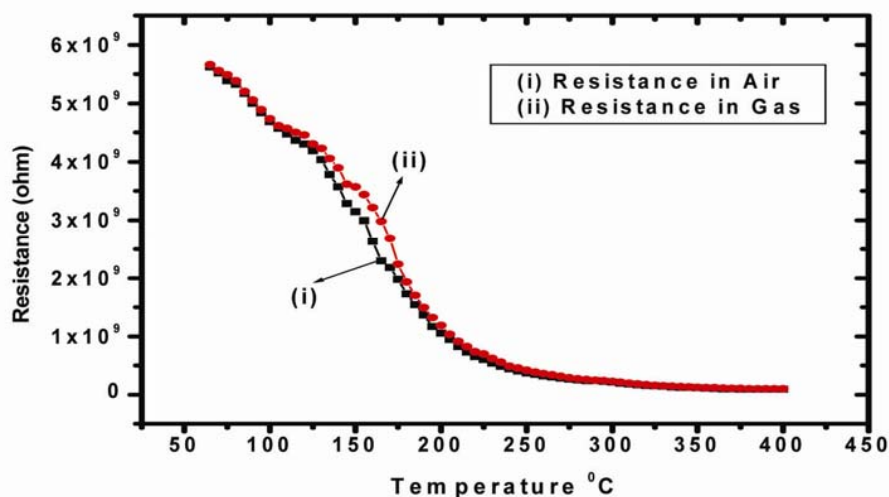


**Fig. (4).** The typical variation of resistance of HAp thick film as a function of temperature. (i) Thick film in the presence of air atmosphere. (ii) Thick film in the presence of CO<sub>2</sub> gas in 1000 ppm.

calcium and the mass % of these elements were found to be 14.22, 45.74, 0.30, 18.23, 21.51 respectively. EDS was carried out to confirm the XRD results and to see occurrence of any impurity which may get incorporated while fabrication of thick films.

### 3.3. Gas Sensing Performance of HAp Thick Film Sensor

Fig. (4) shows typical behavior of resistance for HAp sensor as a function of temperature. Resistance of sensor material decreases at elevated temperature when kept in ambient air as well as in gas atmosphere. Fig. (5a) depicts the variation of the sensitivity factor [SF(%) (R)] as a function of temperature in CO<sub>2</sub> gas atmosphere, with fixed gas concentration of 1000 ppm. It was observed that sensitivity factor remains very low up to 100°C and increases as a function of temperature up to 165°C. It possesses a maximum sensitivity factor of 31.1 at 165°C and decreases further with rise in temperature. Similar behaviour was observed for all the three cycles for sensor film. This indicates that such film can be used as a sensor due to its repeatable behaviour. Fig. (5b) shows the reproducibility of the sensor film wherein second sample (Film 2) was subjected to five cycles. The behavior of second film was found to be completely consistent with that of Film 1. This reveals the reproducibility of the HAp thick film sensor. The repeatability and reproducibility cycles confirmed that HAp thick film can be used as a CO<sub>2</sub> sensor at an optimum temperature of 165°C which is much lower than that reported by Nagai *et al.* [13].

### 3.4 Response and Recovery Times

Fig. (6) represents the variation in sensitivity factor with time in response to 1000 ppm CO<sub>2</sub> gas for the HAp thick film held at 165°C. When the sensor was exposed to gas atmosphere, sensitivity factor (G) was found to increase with time which later on remained constant with further increase in time. Upon exposure to air, the reduction in SF(%) (G) was observed.

The number of cycles of change in SF(%) (R) with time for HAp, when exposed to gas & air alternately is shown in

Fig. (7). From the figure, it can be concluded that the average response time of HAp thick film to CO<sub>2</sub> gas is 20 second, and it was much lower than that reported in literature [13]. The average time needed to have 90% recovery to the original resistance was of the order of 15 seconds.

### 3.5. Active Region of HAp Thick Film Sensor

The change in sensitivity factor with CO<sub>2</sub> gas concentration is presented in Fig. (8). From the figure, it can be concluded that the behavior of SF(%) (R) as a function of gas concentration shows three main regions. The first region shows sharp initial rise in SF(%) up to 1500 ppm (high sensitivity region). The second intermediate region, from 1500 ppm to 9000 ppm, shows nearly linear increase in SF(%), and third region was the saturation region in which the sensor completely saturates (9000 ppm to 14000 ppm). The rate of increase in sensitivity factor was relatively larger up to 9000 ppm. It may be due to the monolayer adsorption of CO<sub>2</sub> gas molecules on the surface that could cover the whole surface of the film. The excess gas molecules can not reach surface active sites of the sensor so the sensitivity factor at higher concentration, due to further exposures of the gas, is not expected to increase further in large extent. Therefore, it can be concluded that the active region of the HAp thick film sensor was, up to 9000 ppm.

### 3.6. Gas Sensing Mechanism

The hydroxyapatite surface can be characterized by unique properties like several P-OH groups &/or several ionic species like Ca<sup>2+</sup>, PO<sub>4</sub><sup>3-</sup> & OH<sup>-</sup> alongwith porosity. The P-OH groups determine the reactivity with gas molecules as they act as adsorption sites for the gas to be sensed. In addition to this, porous network works as a conduction path for adsorbed gas molecules. Thus, there is a wider distribution of adsorption sites available on the surface of HAp.

The OH<sup>-</sup> ions are important for adsorption process. When CO<sub>2</sub> adsorb on HAp surface, it interacts with OH<sup>-</sup> ions according to the following reaction;

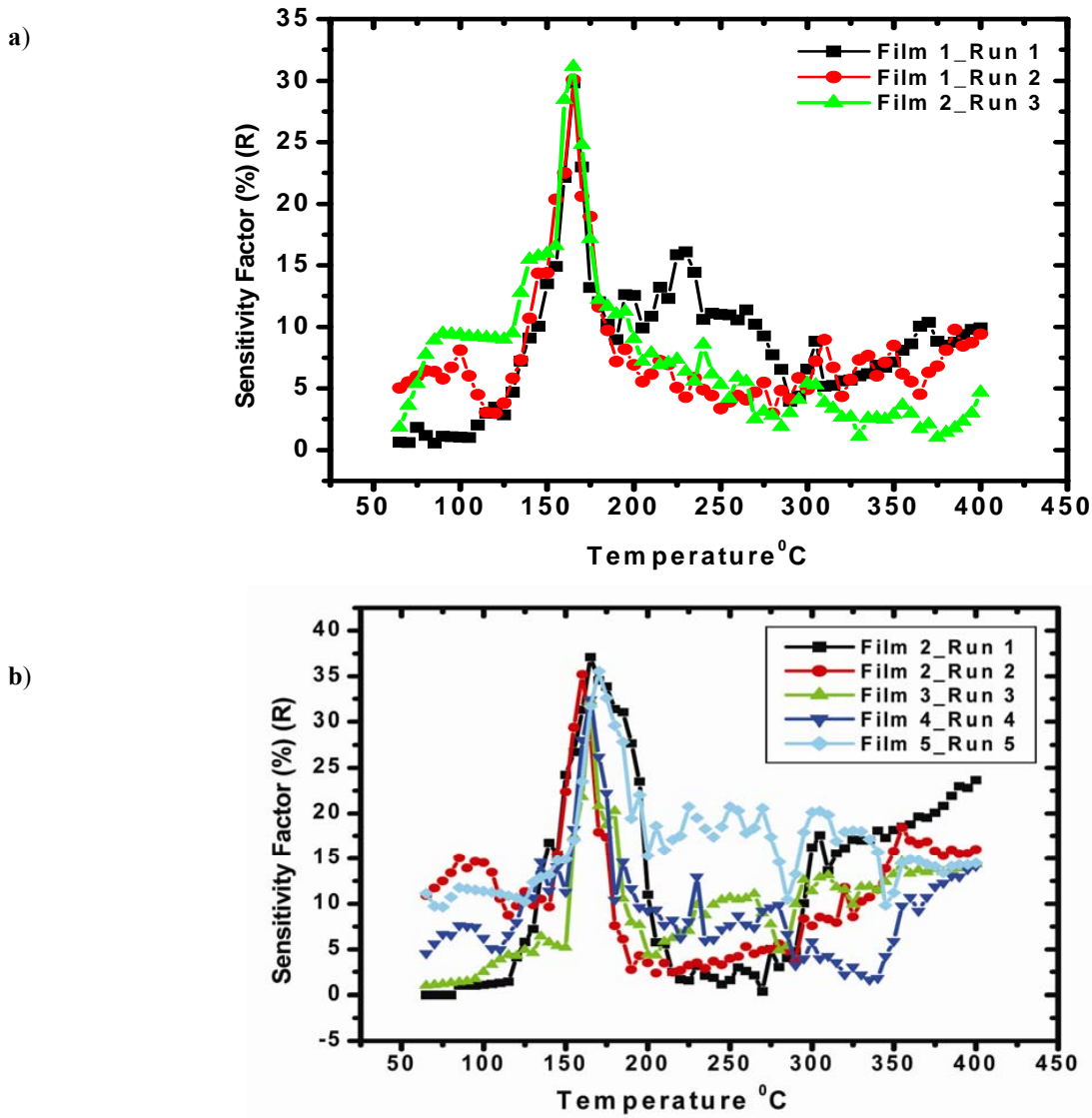


**Fig. (5).** (a) The change in SF(%) (R) of HAp thick film (F1) with variation in temperature for 1000 ppm CO<sub>2</sub> gas concentration. (b) Reproducibility of HAp thick film (F2) showing the change in SF(%) (R) with variation in temperature for 1000 ppm CO<sub>2</sub> gas concentration.

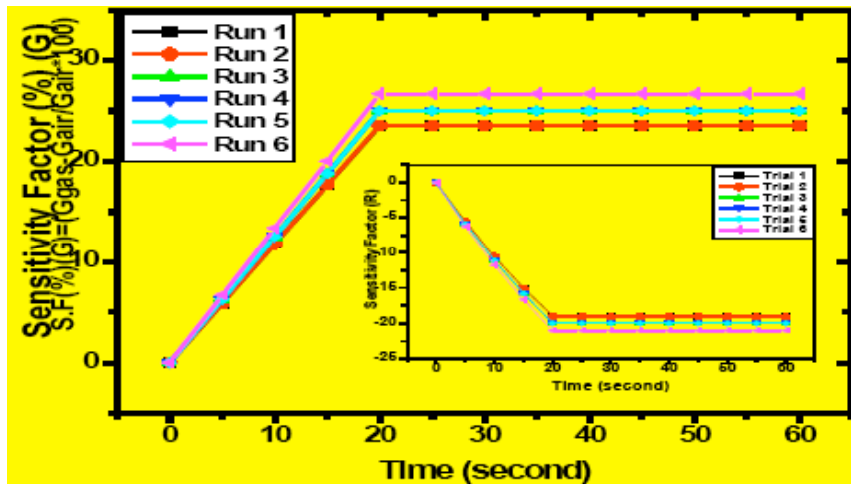


**Fig. (6).** The variation in sensitivity factor (%) (R) for the HAp thick film operated at 165°C as a function of time (sec) in response to 1000 ppm CO<sub>2</sub> gas.

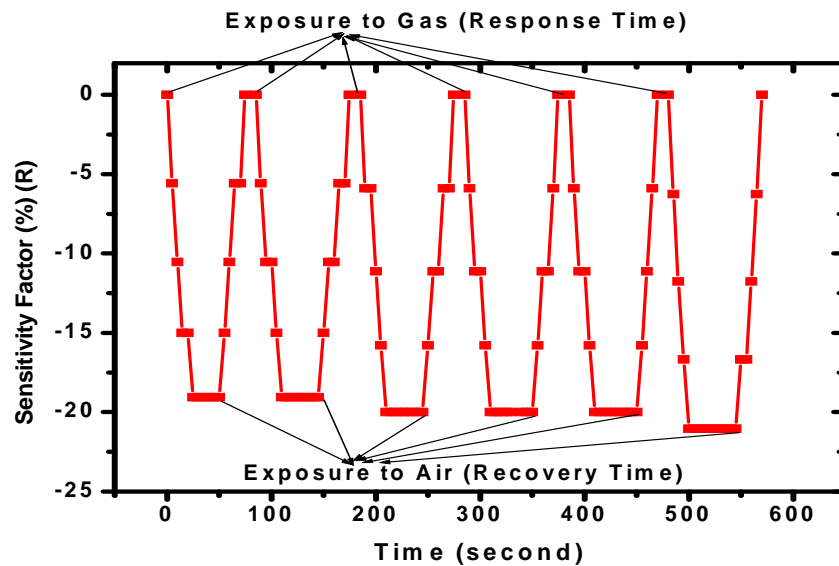


**Fig. (7).** Change in SF(%) (R) of HAp thick film when exposed to gas & air alternately showing response and recovery times for 1000 ppm gas concentration.

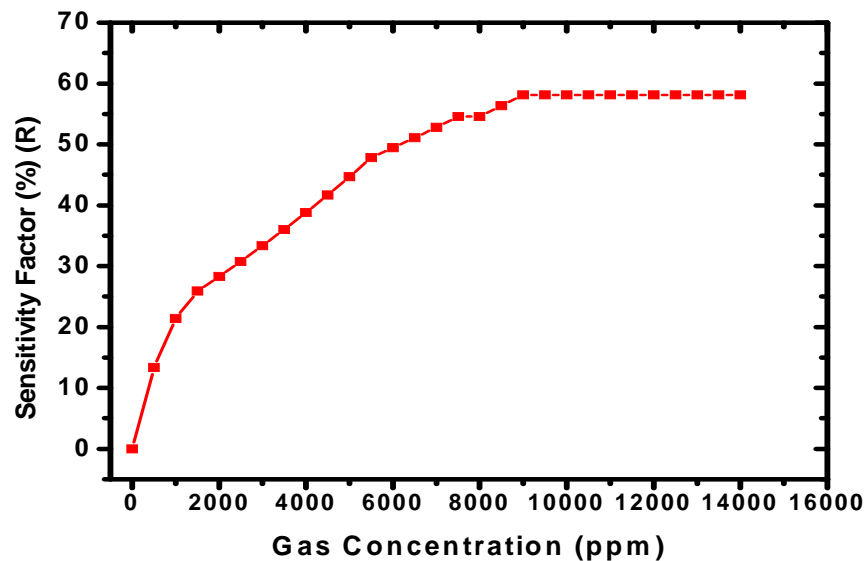


**Fig. (8).** Typical variation in sensitivity factor (%) (R) for HAp thick film as a function of gas concentration for CO<sub>2</sub> at an optimum temperature 165°C.



Thus, the physisorbed CO<sub>2</sub> molecules are converted in to CO<sub>3</sub><sup>2-</sup> ions.

Therefore change in the resistance of the sensor is observed only in the temperature window 100 °C to 200 °C due to CO<sub>2</sub> adsorption. Usually at higher temperatures, the rate of adsorption becomes less dominant than desorption. When the rate of adsorption & rate of desorption becomes equal, sharp increase in the sensitivity factor is observed. Desorption process dominates the adsorption at higher temperatures [12]. From the Figs. (5a) & (5b), it can be revealed that HAp can work as a CO<sub>2</sub> sensor at operating temperature of 165°C.

#### 4. CONCLUSIONS

The HAp thick film is successfully deposited on alumina substrate by using the screen printing technique. The depos-

ited HAp film has shown hexagonal phase with nano-sized grains. The surface morphology of HAp film revealed microcracks, and formation of agglomerates with porosity. Carbon, oxygen, phosphorus and calcium are the elements of HAp film as confirmed by EDS. HAp thick film uniquely detects CO<sub>2</sub> gas at a temperature as low as 165°C. Response and recovery times of HAp thick film CO<sub>2</sub> gas sensor are found to be 20 second and 15 second respectively. Active region for HAp thick film sensor is found to be up to 9000 ppm of gas load. The study concludes that HAp thick film can be used as a CO<sub>2</sub> gas sensor at an operating temperature 165°C.

#### ACKNOWLEDGEMENT

Thanks are due to Hon'ble Vice-Chancellor, Dr S.B. Nimse, SRTM University, Nanded, for his valuable guidance and constant encouragement. The authors would also like to

acknowledge the financial support from DST, New Delhi (F.No.SR/S2/CMP-74/2006).

#### ABBREVIATIONS

EDS	=	Energy Dispersive Spectroscopy
Ga	=	Conductance in air
Gg	=	Conductance in gas
HAp	=	Hydroxyapatite
ppm	=	Parts per million
Ra	=	Resistance in air
Rg	=	Resistance in gas
Rr	=	Reference Resistance
Rs	=	Sensor Resistance
SEM	=	Scanning Electron Microscopy
SF(%) (G)	=	Sensitivity Factor in the form of Conductance
SF(%) (R)	=	Sensitivity Factor in the form of Resistance
Vr	=	Voltage Drop
Vs	=	DC Supply Voltage
XRD	=	X-Ray Diffractometer

#### REFERENCES

- [1] More PS, Kholam YB, Deshpande SB, *et al.* Introduction of  $\delta$ - $\text{Al}_2\text{O}_3/\text{Cu}_2\text{O}$  material for  $\text{H}_2$  gas sensing applications. *Mater Letts* 2004; 58: 1020-5.
- [2] Lee HJ, Kim SE, Choi HW, Kim CW, Kim KJ, Lee SC. The effect of surface-modified nano-hydroxyapatite nano composites. *Eur Polymer J* 2007; 43: 1602-8.
- [3] Kanno T, Sendai T, Tada K, Horiuchi J-I, Akazawa T. Adsorption properties of acidic and basic proteins on the surface of carbonate-containing hydroxyapatite. *Phosphorus Res Bull* 2007; 21: 25-30.
- [4] Motoki E, Ueno S, Shimabayashi S. Effect of ionic surfactants on the adsorption of bovine serum albumin to the surface of hydroxyapatite. *Phosphorus Res Bull* 2007; 21: 9-15.
- [5] Kaneda K, Mori K, Hara T, Mizugaki T, Ebitani K. Design of hydroxyapatite -bound transition metal catalysts for environmentally-benign organic synthesis. *Catal Surv Asia* 2004; 8: 231-9.
- [6] Xia W, Chang J. Well ordered mesoporous bioactive glasses (MBG): a promising bioactive drug delivery system. *J Control Rel* 2006; 110: 522-30.
- [7] Park Y-S, Yamazaki Y. Novel Nafion/Hydroxyapatite composite membrane with high crystallinity and low methanol crossover for DMFCs. *Polymer Bull* 2005; 53: 181-92.
- [8] Fukii E, Kawabata K, Ando K, Tsuru K, Hayaakawa S, Osaka A. Synthesis and structural characterization of silica-hybridized hydroxyapatite with gas adsorption capability. *J Ceram Soc Jpn* 2008; 114(9): 769-73.
- [9] Tanaka H, Chikazawa M, Kandori K, Ishikawa T. Influence of thermal treatment on the structure of calcium hydroxyapatite. *Phys Chem* 2000; 2: 2647-50.
- [10] Mahabole MP, Aiyer RC, Ramakrishna CV, Sreedhar B, Khairnar RS. Synthesis characterization and gas sensing property of hydroxyapatite ceramic. *Bull Mater Sci* 2005; 28(6): 535-45.
- [11] Mahabole MP, Pillai PM, Aiyer RC, Khairnar RS. Dielectric and gas sensing property of hydroxyapatite nano-ceramic. In: *Proceedings of International conference on Advances in Materials, Product design and Manufacturing Systems (ICMPM 2005)*. Bannari Amman Institute of Technology, Tamil Nadu, 2005.
- [12] Mahabole MP, Sonawane Y, Inamdar A, Aiyer RC, Khairnar RS. Hydroxyapatite as a CO gas sensor. *SENSOR-10*. In: *Proceedings of 10<sup>th</sup> National Seminar on Physics and Technology of Sensors*, VIT, Pune, 2004.
- [13] Nagai M, Nishino T, Saeki T. A new type of  $\text{CO}_2$  gas sensor comprising porous hydroxyapatite ceramics. *Sens Actuators* 1988; 15: 145-51.
- [14] Cheng H, Yasukawa A, Kandori K, Ishikawa T. FTIR study on incorporation of  $\text{CO}_2$  into calcium hydroxyapatite. *J Chem Soc Faraday Trans* 1998; 94(10): 1501-5.
- [15] Wang B, Zhang J-J, Pan Z-Y, Tao X-Q, Wang H-S. A Novel hydrogen peroxide sensor based on the direct electron transfer of horseradish peroxidase immobilized on silica-hydroxyapatite hybrid film. *Biosens Bioelectron* 2009; 24: 1141-5.
- [16] Silva CC, Almedida AFL, De Oliveira RS, Pinheiro AG, Goes JC, Sombra ASB. Dielectric permittivity and loss of hydroxyapatite screen-printed thick films. *J Mater Sci* 2003; 38: 3713-20.
- [17] Almeida AFL, Fachine PBA, Sasaki JM, *et al.* Optical and electrical properties of barium titanate-hydroxyapatite composite screen-printed thick films. *Solid State Sci* 2004; 6: 267-78.

Received: March 20, 2009

Revised: September 05, 2009

Accepted: September 15, 2009

© Mene *et al.*; Licensee *Bentham Open*.

This is an open access article licensed under the terms of the Creative Commons Attribution Non-Commercial License (<http://creativecommons.org/licenses/by-nc/3.0/>) which permits unrestricted, non-commercial use, distribution and reproduction in any medium, provided the work is properly cited.